Physica C 206 (1993) 335-344
North-Holland

PHYSICA C

Pulse $I-V$ characteristics measurement to study the dissipation mechanism in epitaxial $YBa_2Cu_3O_x$ thin films at high current densities

S.K. Gupta [a,1], P. Berdahl [a], R.E. Russo [a], G. Briceño [b] and A. Zettl [b]

[a] Energy and Environment Division, Lawrence Berkeley Laboratory, Berkeley, CA 94720, USA
[b] Department of Physics, University of California at Berkeley, and Materials Sciences Division, Lawrence Berkeley Laboratory, Berkeley, CA 94720, USA

Received 4 November 1992
Revised manuscript received 15 December 1992

A simple pulse method of measuring current-voltage characteristics ($I-V$) at high current densities is described. We report $I-V$s on epitaxial $YBa_2Cu_3O_x$ thin films at high current densities in the presence of a magnetic field parallel to the c-axis. The results show that the Bardeen-Stephen flux flow model does not account for dissipation at high current densities in $YBa_2Cu_3O_x$ thin films. In the presence of a magnetic field, we find qualitative agreement with a simple theoretical model based on dissipation caused by 2D vortices excited from the flux lines. In the absence of a magnetic field, a power law behavior arises due to current-induced depairing of thermally excited 2D vortices.

1. Introduction

The dissipation mechanism in high-T_c superconductors is not well understood. This is in contrast to conventional superconductors where dissipation is reasonably well understood on the basis of the Anderson-Kim flux creep model at low current densities and the flux flow model at high current densities [1-3]. Current-voltage ($I-V$) characteristics of thick films and polycrystalline $YBa_2Cu_3O_x$ samples reportedly show flux creep behavior at low currents and a linear flux flow region similar to conventional superconductors at high currents [4,5]. This behavior, however, can be attributed to dissipation in the inter-granular region. $I-V$ measurements have also been carried out on epitaxial high-T_c thin films and single crystals by many groups [1,6-11]. Various models, such as conventional flux creep [1,6], vortex glass transition [7,10], resistance due to the flow of 2D vortices and the Kosterlitz-Thouless transition [8,9,11] etc., have been used to explain the obtained results. These measurements, however, have been done at low current densities. Measurements at high current densities have been limited by heating effects which cause the destruction of the bridge used in thin film measurements. It has been believed [1,12,13] that high current dissipation will be limited by flux flow leading to linear $I-V$s.

This study was undertaken to make measurements at current levels where linear $I-V$s are expected, in order to probe the flux flow regime in these materials. To overcome thermal runaway conditions a repetitive pulsed method using very simple equipment has been employed. Previous experiments on single crystals and epitaxial films have used DC or a low frequency current sweep [7] which cause strong heating effects at high currents. Some studies using repetitive pulse measurements of $I-V$ characteristics have also been reported on polycrystalline bulk material and thick films [5,15]. Single pulse methods have also been used for J_c measurements [14]. We describe a much simpler method utilizing lock-in amplifiers and a pulse generator. Limitations of the maximum power densities that can be dissipated

[1] Permanent address: Technical Physics and Prototype Engineering Division, Bhabha Atomic Research Centre, Bombay-400085, India.

during pulse measurements on thin films are also discussed. We report I–V characteristics of two $YBa_2Cu_3O_x$ thin films over a wide temperature range in a magnetic field along the c-axis up to 6 T. The I–Vs show a power law behavior at all temperatures and magnetic fields. These results indicate that $YBa_2Cu_3O_x$ thin films do not exhibit a conventional flux flow dissipation. A power law behavior at low current densities in the presence of a magnetic field has been reported earlier [6,8,9,11]. This behavior in $YBa_2Cu_3O_x$ thin films has been explained in the framework of a flux creep model with a pinning energy dependent on current, magnetic field and temperature. For BSCCO single crystals [8] a model based on dissipation caused by 2D vortices excited from flux lines has been used to explain a similar behavior in fields up to 1 kG. This model excludes the effect of Josephson interlayer coupling which is small for BSCCO. We explain our results at high current densities using a similar model which includes Josephson coupling between superconducting layers. We find that the magnetic field dependence of the power law exponent is in qualitative agreement with this model. We believe that an accurate calculation of the interaction between 2D vortices and flux lines could help to clarify the dissipation in the mixed state in high-T_c materials.

2. Flux flow model

According to the flux flow model [3,16], at high current densities the Lorentz force on flux lines penetrating through the sample exceeds the pinning forces and vortices move in a steady motion at a velocity limited by viscous drag. In this region the I–V characteristics are linear and can be expressed as

$$V = R_f(I - I_c)\,, \tag{1}$$

where I_c is a constant and R_f is the flux flow resistance. R_f depends on the magnetic field (B), the sample resistance in the normal state (R_n) and temperature (T), and can be expressed as

$$R_f = R_n(B/H_{c2})f(T/T_c, B/H_{c2})\,, \tag{2}$$

where H_{c2} is the value of the upper critical magnetic field at zero temperature and T_c is the critical temperature in zero magnetic field. The value of f is about 1 at low temperatures ($T/T_c \ll 1$) or at low magnetic fields ($B/H_{c2} \ll 1$) [3]. Since H_{c2} for $YBa_2Cu_3O_x$ along the c-axis is estimated to be ≈ 60 T and we used a magnetic field of less than 6 T, we expect a flux flow resistance almost independent of temperature (except very close to T_c) given by

$$R_f = R_n B/H_{c2}\,. \tag{3}$$

3. Heating effects during pulse measurements

We now estimate the temperature rise in a thin film bridge during a pulse measurement. We consider a thin film bridge of length L and width W prepared on a substrate with thermal conductivity k and specific heat c_p. The current and voltage contacts are assumed to be far from the bridge so that the heat from them does not reach the bridge during application of the current due to the short duration of the pulse. Upon application of the pulse, heat is dissipated in the bridge at the rate of $P = IV$ for a time t_0 (duration of the pulse) and its temperature rise consists of two parts:
(1) a temperature drop ΔT_1 across the thermal boundary resistance [17] between film and substrate, and
(2) a temperature rise ΔT_2 at the top surface of the substrate below the film due to heat flow in the substrate.
These can be treated independently since the thermal response time of the boundary layer is much shorter (~ns) than the heat diffusion time in the substrate.

The temperature drop across the thermal boundary resistance [17] is given by

$$\Delta T_1 = R_{bd}P/A\,, \tag{4}$$

where $A = L\,W$, is the area of the bridge, and R_{bd} is the thermal boundary resistance. It should be noted that ΔT_1 at a given current density is independent of area. Furthermore, it increases to a steady state value within a few nanoseconds of the application of the pulse. The value of R_{bd} is nearly independent of the substrate and is approximately 10^{-3} K cm^2/W according to ref. [17]. In these experiments we have used bridges of width 25 μm and lengths varying between 250 and 600 μm. For a 600 μm bridge the peak power, where heating effects were seen, is of the order of 6 mW. For these parameters we get $\Delta T_1 \sim 0.04$ K (from eq. (4)) as the temperature rise due to the boundary resistance.

Since the three-dimensional heat diffusion equation for the sample geometry cannot be solved exactly, we will estimate the temperature rise of the film due to heat flow in the substrate. In a time t after the application of a pulse, heat diffuses a distance d in the substrate which is given by $d \sim 2(Dt)^{1/2}$, where $D = k/c_p$ is the heat diffusion constant. This is schematically shown in fig. 1. The volume in which heat diffuses is $V \cong (2d + W)dL$. The average temperature rise of this volume is therefore $Pt/(Vc_p)$. The temperature rise at the surface of the substrate will be higher than the average temperature rise by a factor α and may be written as

$$\Delta T_2 = \alpha Pt / \{2L(Dt)^{1/2}[4(Dt)^{1/2} + W]c_p\} . \qquad (5)$$

In order to estimate α we compare this relation (when $W \gg (Dt)^{1/2}$) with the temperature rise at the surface of a semi-infinite solid at constant heat flow. The heat diffusion equation in this case can be solved exactly [18] to yield an approximate value of $\alpha = 4/(\pi^{1/2})$. For $SrTiO_3$ substrates, the thermal constants have the values of $c_p = 1$ J/K cm^3, $k = 0.18$ W/K cm, $D = K/c_p \cong 0.18$ cm^2/s at 80 K [19]. Using a typical maximum pulse power of $P = 6$ mW for a 25 µm wide and 600 µm long bridge, we get a temperature rise $\Delta T_2 = 0.13$ K at the end of a 50 µs pulse. This gives a total temperature rise of 0.17 K at the end of a 6 mW pulse.

We now consider whether the measurement could be made at still higher power densities with similar temperature rises. Measurements at higher power densities could be made by reducing W or the pulse width t_0. This increase in power density, however, is limited to about a factor of 4 due to the enhancement of the ΔT_1 term. Still higher power densities could be achieved only by reducing the thickness of the film. It should be noted that the use of a substrate with better thermal conductivity does not help since the boundary layer resistance is almost independent of the substrate [17].

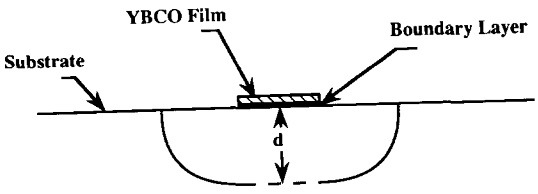

Fig. 1. Heat flow in the sample.

4. Experimental

Thin films of $YBa_2Cu_3O_x$ were deposited using a KrF (248 nm) excimer laser deposition system as described earlier [20]. Briefly, a $YBa_2Cu_3O_x$ target was used and deposition was carried out in situ at 750°C on (100) oriented $SrTiO_3$ substrates of 1.0 mm thickness. Films were well oriented, as only the peaks corresponding to the c-axis normal to the substrate were observed in X-ray diffraction. Two films were used for this study, film A (20 nm thick) was patterned to 25 µm×600 µm, and film B (70 nm thick) was patterned to 25 µm×350 µm. Their critical current densities at 77 K for $B = 0$ and 0.4 T parallel to the c-axis are 1.6 and 0.6×10^6 A/cm^2, respectively. For electrical measurements, the sample was mounted on a small copper block making good thermal contact and four probe contacts were made using silver paint. The samples were cooled using a liquid helium cryostat and a magnetic field normal to the substrate was applied using a superconducting magnet. Some measurements were done by using a closed cycle helium cryostat and a permanent magnet. The temperature of the sample could be controlled to within 0.02 K.

Figure 2 shows the resistance of film A as a function of temperature without an applied magnetic field. We can observe the metallic-like behavior and the sharp superconducting transition at $T_c \approx 89$ K, which characterize a good quality $YBa_2Cu_3O_x$ thin film.

Figure 3 shows the circuit used to measure the I–V characteristics of our thin films. A pulse generator was used to give pulses of up to 5 V amplitude and 50 µs duration. Pulses were separated by 5 ms, giving a duty cycle of 1%. The current during the measurement was controlled using a resistance R and the voltage control from the pulse generator. The peak voltage generated by this current in the sample was measured using a Model 5204 Princeton Applied Research lock-in amplifier. This lock-in amplifier

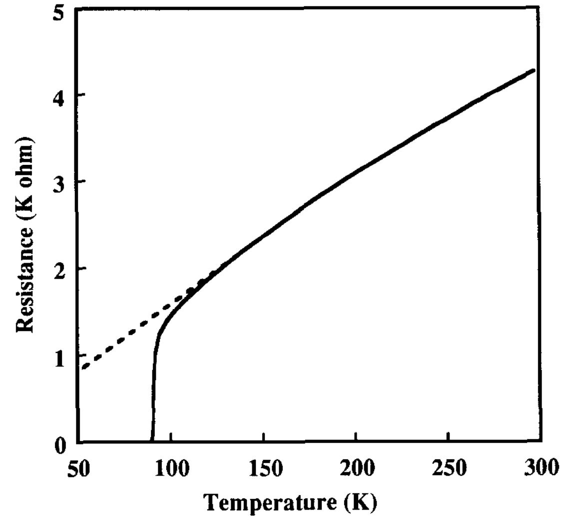

Fig. 2. Resistance vs. temperature plot for sample A. The dotted line indicates the extrapolated normal resistance at temperatures below the transition temperature.

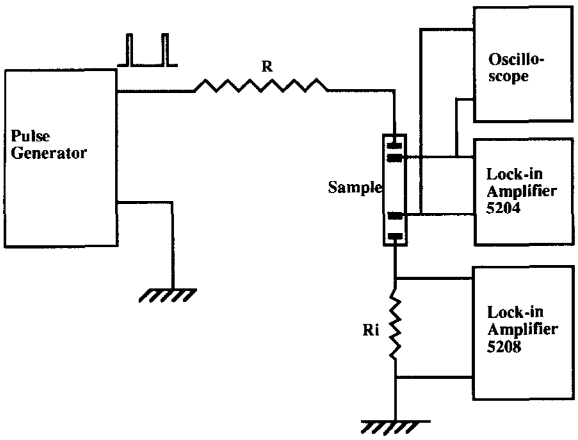

Fig. 3. Circuit diagram for pulse I–V measurement.

uses a square wave signal as a reference and responds to fundamental and odd harmonics. When used in wide band mode, it gives an output which depends on the average absolute voltage, for the shape of pulses used. The peak current was measured by measurement of voltage across resistance R_i using a PAR lock-in amplifier Model 5208. This lock-in amplifier responds only to the fundamental frequency. However, for a fixed shape of the signal, the response is proportional to the pulse amplitude. The calculated values of the peak amplitude from the measurements on both lock-in amplifiers were in agreement with those directly measured using an oscilloscope. However, an accurate I–V characteristics measurement cannot be made using a simple analog oscilloscope as the accuracy of measurement in that case is limited to nearly 5%. On the other hand, using a lock-in amplifier, measurements can typically be made with 0.1% accuracy.

Heating effects in the film could be seen by sharp changes in current and voltage pulse shape as shown in fig. 4. Both current and voltage pulses changed shape as the resistance R in series with the pulse generator was of the same order as the sample resistance at high currents. These heating effects were observed at fairly well-defined current levels and occurred at a peak power of nearly 6 mW for the 600 μm long bridge. No changes in the sample temperature were detected by a temperature sensor mounted in the copper block due to the small average power used. In order to find any possible errors in the pulsed measurement, DC I–V characteristics were compared to pulsed I–Vs for a sample. The results indicate good agreement between the two measurements as seen in fig. 5(a). It may be noted that DC measurements at higher currents are limited by heating effects and pulse measurements at low voltages

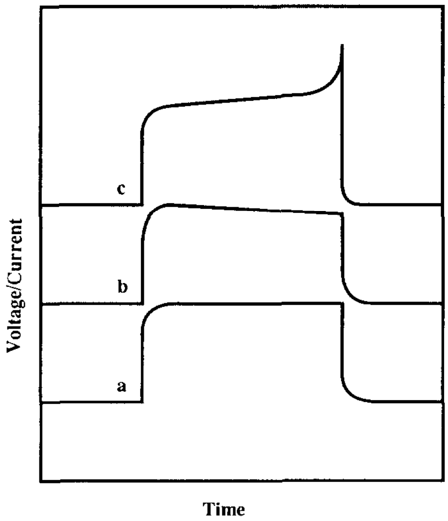

Fig. 4. Shape of the current and voltage pulses. (a) Current or voltage pulse at low power density and (b) current and (c) voltage pulses at high power density.

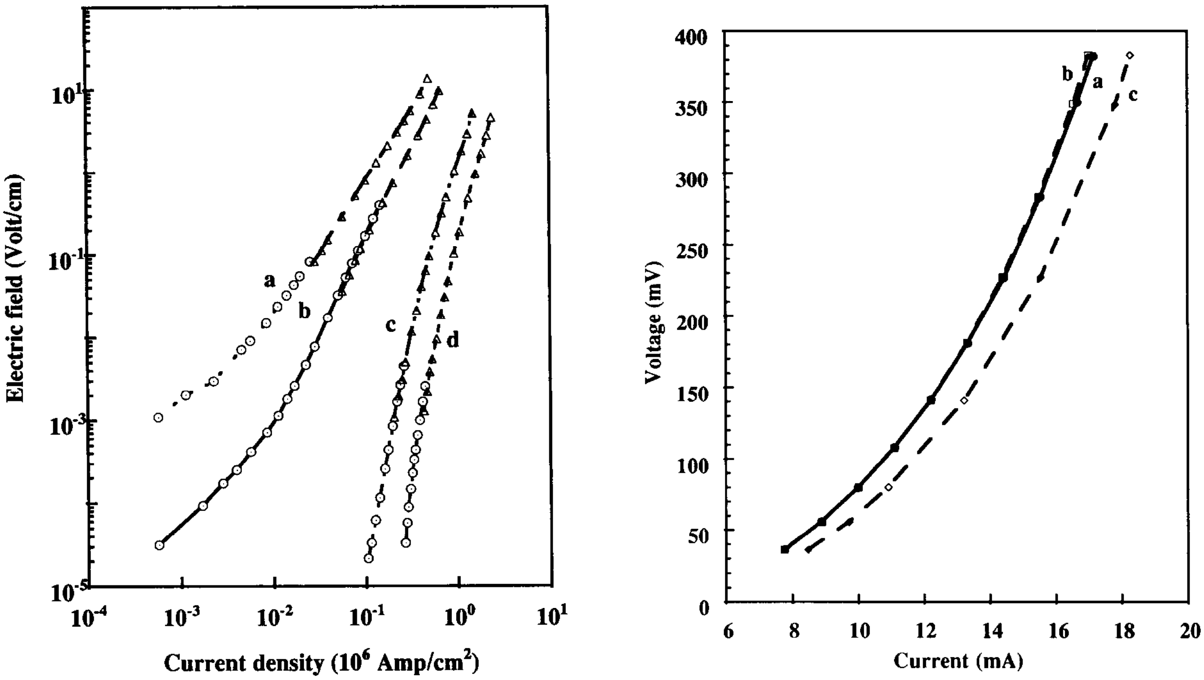

Fig. 5.(a) Comparison of DC and pulse measurements of the I–V characteristics of a thin film bridge in a 0.4 T field. Measurements made at temperatures of (a) 90.0 K, (b) 89.0 K, (c) 82.5 K and (d) 75.5 K. Circles and triangles indicate data points obtained by DC and pulse measurements, respectively. (b) Effect of pulse width and temperature on the I–V characteristics of a thin film bridge, (a) 50 μs pulses at 87.1 K, (b) 100 μs pulses at 87.1 K and (c) 50 μs pulses at 86.7 K.

are limited by noise. The noise in pulse measurements is increased relative to the signal as the duty cycle of the signal is 1% and therefore the lock-in amplifier response is roughly 1% of the peak signal amplitude being measured. In order to ensure that heating effects are indeed small, measurements were also made on a sample at 86.7 K and 87.1 K using a normal pulse width (50 μs) and also at 87.1 K using a pulse width twice as large (100 μs) keeping the same pulse separation. The results shown in fig. 5(b) indicate that pulse heating effects, up to the maximum peak power used, correspond to an average temperature change in 50 μs of less than 0.1 K, in agreement with the above calculations. During our measurements it became clear that using a DC current would have destroyed the bridge due to thermal runaway. However, during a pulsed measurement a peak power much higher than 6 mW (the power level where heating effects are first seen) did not change the bridge characteristics.

5. Results and discussion

I–V characteristics of film A were measured at various temperatures between T_c and 56 K. The measurements were made in a magnetic field of 0.4 T applied along the c-axis. Figure 6 shows the results, which follow a power law ($V \sim I^a$) behavior with exponent increasing with decreasing temperature. The measurements were made up to a dV/dI of 390 Ω (resistivity = 32.5 μΩ cm) at 85.90 K and 18 Ω (resistivity = 1.5 μΩ cm) at 65.96 K and no linear region in the I–V characteristics was identified. The expected flux flow resistance of this sample from eq. (3) varies between 8.3 and 6 Ω at these temperatures, using the extrapolated normal resistance from fig. 2 (we have used the value of H_{c2} = 60 T [21]). This shows that dissipation at high currents in epitaxial $YBa_2Cu_3O_x$ films is not limited by flux flow and therefore some other mechanism must be responsible for the higher dissipation observed. This is in contrast to the flux flow regime seen in $YBa_2Cu_3O_x$

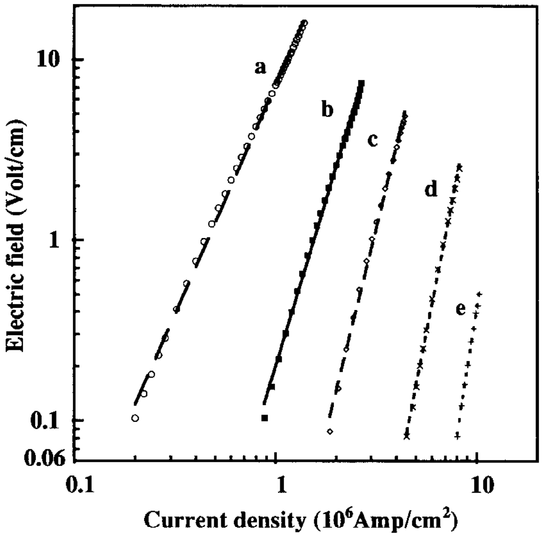

Fig. 6. I–V curves for sample A in a 0.4 T magnetic field plotted as electric field vs. current density at (a) 85.90 K, (b) 80.96 K, (c) 76.07 K, (d) 65.96 K and (e) 55.92 K.

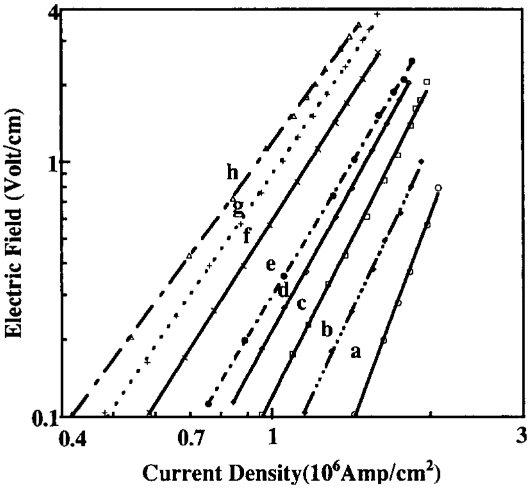

Fig. 7. I–V curves for sample B plotted as electric field vs. current density at 80.61 K in magnetic fields of (a) 0.5 T, (b) 1.0 T, (c) 1.5 T, (d) 2.0 T, (e) 2.5 T, (f) 3.5 T, (g) 4.5 T and (h) 6.0 T.

polycrystalline samples [5], which could be due to flux flow in the intergranular region. To further investigate the absence of a flux flow region, a second sample (sample B) was studied. The I–Vs exhibited a power law behavior again, in all measurements made, as a function of temperature and magnetic field up to 6 T. Figure 7 shows I–V curves in a log-log plot as a function of magnetic field at 80.6 K. Notice that the dissipation increases and the power law exponent decreases as the magnetic field is increased.

Within the framework of conventional theories for dissipation in superconductors, the observed absence of a flux flow region in $YBa_2Cu_3O_x$ thin films could arise because of strong pinning forces compared to the Lorentz force at temperatures and magnetic fields used for measurement. Dissipation in this case will be caused by flux creep. Alternatively the absence of flux flow could be caused by some other mechanism of dissipation being dominant compared to flux creep and flux flow. In what follows we analyze our results based on dissipation caused by 2D vortices in superconducting layers.

The power law I–V characteristic behavior in zero field has been observed in various high-T_c superconductors [8,9,11]. These materials are layered superconductors with weak coupling between the layers. The power law behavior has been explained [22,23] by current-induced depairing of thermally excited 2D vortex pairs in these layers. Some evidence for a Kosterlitz–Thouless (K–T) transition, with a jump of the power law exponent from 1 to 3, caused by thermal dissociation of these pairs has also been observed in $YBa_2Cu_3O_x$ thin films and single crystals [24–26]. In fig. 8 we show our measurement of the variation of the exponent with temperature at selected magnetic fields. In particular, at zero field, we do not observe the predicted K–T exponent jump (from 1 to 3) at the transition temperature. This could be due to fluctuations [9] and the effect of interlayer coupling on the K–T transition as discussed in ref. [23]. The increase of the power law exponent with decreasing temperatures and its approximate linear behavior near T_c are, however, in agreement with dissipation caused by current-induced unbinding of 2D vortices [28].

A model for I–Vs with a power law behavior in magnetic fields has been proposed by Artemenko et al. [8]. This model is based on dissipation due to 2D vortices which are detached from magnetic flux lines. The model, however, neglects the Josephson coupling between the superconducting layers, which may be significant for $YBa_2Cu_3O_x$. We now describe a simple model, which includes the effect of Josephson coupling, similar to that reported in ref. [22] for the

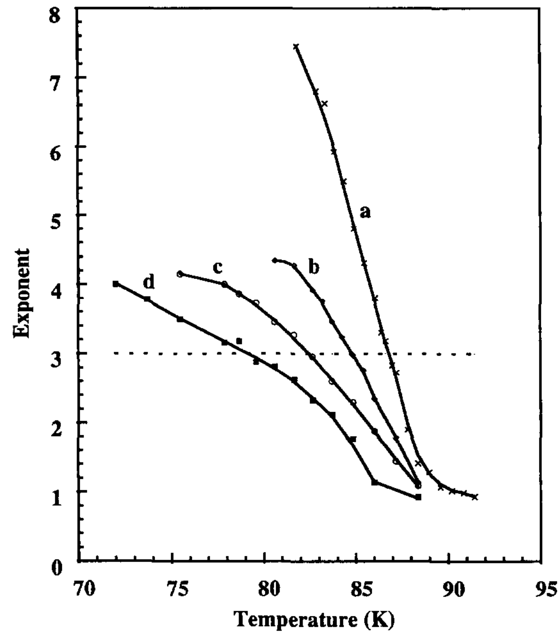

Fig. 8. Variation of the exponent with temperature for sample B in (a) zero field, and in magnetic fields of (b) 1.0 T, (c) 2.5 T and (d) 6.0 T. The dotted line indicates the value of the exponent expected at the K–T transition. Curves are plotted to guide the eye.

zero field case. The model accounts for the power law behavior in magnetic fields at higher current densities, as we have observed, and also explains qualitatively the magnetic field dependence of the exponent.

A flux line in a layered superconductor in a magnetic field may be considered to be a superposition of 2D vortices in individual layers [27], interacting by Josephson coupling and magnetic interaction [23]. These 2D vortices can be separated from each individual flux line by thermal fluctuations and the presence of a Lorentz force. The interaction energy between such a 2D vortex at a distance r from its flux line and the rest of the flux line may be written [23] as the sum of an interaction energy due to magnetic interaction and that due to Josephson coupling between the layers.

The magnetic interaction energy $U_1(r)$, neglecting the effect of other flux lines, is given [8,27] by

$$U_1(r) = Ak_B T(r/2\lambda)^2 \ln(2\lambda/r) \qquad \text{at } r \ll \lambda , \qquad (6a)$$

and

$$U_1(r) = Ak_B T \ln(r/2\lambda) \qquad \text{at } r \gg \lambda , \qquad (6b)$$

where λ is the penetration depth for currents in the a–b plane and $A = \Phi_0 d(4\pi\lambda)^{-2}(k_B T)^{-1}$ is a temperature-dependent parameter, Φ_0 is the flux quantum and d is the layer spacing. The effect of a magnetic field on this energy at large distances has been calculated by Artemenko et al. [8] in the case where there is no Josephson coupling. They found the interaction energy to be reduced due to screening by magnetic field lines by a factor of

$$\epsilon = 1 + 16\pi N\lambda^2/\ln A ,$$

where N is the number of vortex lines per unit area. In the presence of strong Josephson coupling this factor will be modified and we may write

$$\epsilon = 1 + \beta(T)B , \qquad (7)$$

where β is a temperature-dependent parameter to be evaluated later. The Josephson coupling energy between a 2D vortex and the flux line from which it is separated is equal to that between the vortex and an antivortex in position of the flux line [23]. This energy at large distances is given [22] by Er/ξ, where ξ is Ginzburg–Landau coherence length in the ab-plane and E is a constant. Due to the presence of a magnetic field this interaction energy is reduced and the Josephson coupling energy term at large distances may be written as $U_2(r) = \alpha_1 Er/\xi$, where α_1 takes into account the reduction of the coupling due to the field. The Josephson coupling energy at short distances is approximately given [23] by

$$U_2(r) = Ak_B T(r/\alpha_0 d)^2 \ln(\alpha_0 d/\xi), \qquad \xi \ll r \ll \alpha_0 d ,$$

where $\alpha_0 = (m_c/m_{ab})^{1/2}$, m_c is the effective mass of the electrons for motion along the c-axis and m_{ab} for motion along the ab-plane, and d is the distance between superconducting layers.

The total interaction energy between a 2D vortex and the rest of the flux line may now be written as

$$U(r) = Ak_B T(r/2\lambda)^2 \ln(2\lambda/r) + A(T)k_B T(r/\alpha_0 d)^2 \ln(\alpha_0 d/\xi), \qquad \xi \ll r \ll \alpha_0 d , \qquad (8a)$$

and

$$U(r)=Ak_BT\ln(r/2\lambda)/\epsilon+\alpha_1 Er/\xi, \qquad r\gg\lambda . \tag{8b}$$

We will now calculate the form of the I–V curves due to the separation of the 2D vortices from the field lines using a standard method as given in refs. [8,22,28]. In the presence of a current density J parallel to the ab-plane there is a force on each 2D vortex given by $F=J\Phi_0 d/c$, where d is the length of the 2D vortex. Therefore the interaction energy (at large distances) in the presence of the current is modified to

$$U(r)=Ak_BT\ln(r/2\lambda)/\epsilon+(\alpha_1 E/\xi-J\Phi_0 d/c)r, \quad \text{at } r\gg\lambda . \tag{9}$$

We will later show that the relation of the interaction energy for $r>\lambda$ is important in the current range used for measurement of the I–V characteristics. This interaction energy of a 2D vortex with the rest of the field line has a maximum at

$$r_c=(AkT/\epsilon)(J\Phi_0 d/c-\alpha_1 E/\xi)^{-1} . \tag{10}$$

The energy at r_c is given by

$$U(r_c)=A(T)k_BT\epsilon^{-1}(\ln r_c/2\lambda-1) .$$

Assuming a classical escape rate of the 2D vortices from the flux lines [28], the rate of separation of the 2D vortices from the flux lines may be written as

$$\Gamma_e\sim N\exp[-U(r_c)/k_BT]\sim N(2\lambda/r_c)^{A/\epsilon} . \tag{11}$$

Using the value of r_c we find

$$\Gamma_e\sim\{(J-J_1)/J_0\}^{A/\epsilon} ,$$

where $J_1=Ec\alpha_1(\xi\Phi_0 d)^{-1}$ and $J_0=Ak_BTc/(2\lambda\epsilon\Phi_0 d)$. In the steady state, the number of 2D vortices depends on the rate of production (Γ_e) and the rate of recombination (proportional to the number of 2D vortices and the number of flux lines with missing 2D vortex in the same plane) and may be written as $n\sim\Gamma_e^{1/2}$. The electrical resistance arises due to the flow of these 2D vortices as they interact with the applied current. Therefore

$$R\sim n\sim\Gamma_e^{1/2}\sim[(J-J_1)/J_0]^{A/2\epsilon} ,$$

and the voltage across the sample can be written as

$$V\sim J[(J-J_1)/J_0]^{A/2\epsilon} .$$

It should be noted that, in this model, J_1 has the physical significance of being the critical current density. At high current densities compared to J_1, we obtain a power law behavior of the I–V characteristics $V\sim J^a$ with the exponent a given by

$$a(B)-1=\frac{A}{2\epsilon}=\frac{A}{2(1+\beta B)} .$$

If a_0 is the value of the exponent in the absence of a magnetic field, then

$$a(B)=1+\frac{a_0-1}{1+\beta B} . \tag{12}$$

In order to estimate the parameter β in this expression we use the model proposed by Artemenko et al. [8] taking into account the Josephson interaction energy term. In this model, the effect of screening is described by a dielectric constant which depends on magnetic field and on the interaction energy of the 2D vortices. The polarizability (α) due to a magnetic field is given [8] by

$$\alpha=\frac{NA\int\exp[-U(r)/k_BT]r^3\,\mathrm{d}r}{2\int\exp[-U(r)/k_BT]r\,\mathrm{d}r} . \tag{13}$$

The shifts of the 2D vortices from their flux lines (causing polarization), due to interaction with a distant 2D vortex whose interaction energy we desire, are small. Therefore, we use the relation of the interaction energy $U(r)$ at small distances in order to evaluate α in eq. (13). Using typical parameters for $YBa_2Cu_3O_x$ we find from eq. (8a) that the Josephson interaction energy term is much larger [23] than the magnetic interaction energy term. We may therefore use the Josephson interaction energy relation to estimate α in eq. (13). Since the Josephson interaction energy relation is approximate we expect an order of magnitude estimate of β from our calculations. Neglecting the magnetic interaction we can evaluate eq. (13) to give

$$\alpha=N\alpha_0^2 d^2/[2\ln(\alpha_0 d/\xi)] .$$

The dielectric constant ϵ [8] may now be written as

$$\epsilon=1+4\pi\alpha=1+2\pi N\alpha_0^2 d^2/\ln(\alpha_0 d/\xi) . \tag{14}$$

Comparing this with eq. (7) we get

$$\beta=2\pi\alpha_0^2 d^2\Phi_0^{-1}/\ln(\alpha_0 d/\xi) . \tag{15}$$

Using typical values of the parameters for $YBa_2Cu_3O_x$

($\alpha_0=5$, $d=1.2$ nm, $\xi=1.5$ nm at low temperatures) we get $\beta=0.4$ T^{-1} at 80 K.

We will now estimate the value of currents up to which the form of the interaction energy at large distances as given in eq. (9) may be used to describe the $I-V$ characteristics. From eq. (9) we find that $r_c>\lambda$ if $J<2J_0=2k_BTc(A/2\epsilon)/(\lambda\Phi_0 d)$; using the typical values of $\lambda=140$ nm and $T=80$ K we find $r_c>\lambda$ for $J<0.7(a-1)\times10^6$ A/cm^2, where a is the exponent of the $I-V$ curves. Using experimental values of a for various $I-V$ curves we see that this condition is approximately satisfied for the measurements reported here.

In fig. 9 we show the magnetic field dependence of the power law exponent at two different temperatures. The solid lines indicate the expected field dependence using eq. (12) of the above model with β used as the only adjustable parameter. The variation of the exponent with field is seen to be in qualitative agreement with the above model. Experimental values of β to yield a best fit to data at 80.61 K and 86.01 K are 0.81 T^{-1} and 2.1 T^{-1}, respectively. This may be compared with the estimate of 0.4 T^{-1} at 80 K made earlier. This agreement may be considered good in view of the fact that the relation for Josephson interlayer coupling at short distances used to calculate β is very approximate.

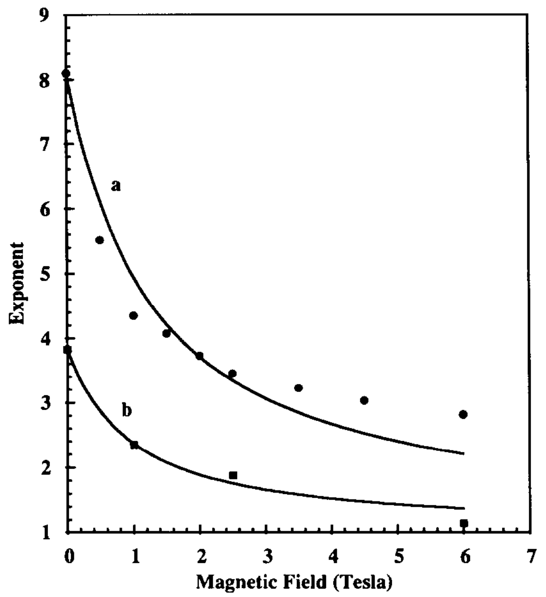

Fig. 9. Variation of the exponent with magnetic field at temperatures of (a) 80.61 K and (b) 86.01 K. Points indicate experimental data and the curves indicate the expected theoretical variation.

6. Conclusion

A pulse method of measuring the $I-V$ characteristics using simple equipment has been described and the limitations of this method on thin films have been reported. The method should be useful for critical current measurements in bulk samples. Measurements of the $I-V$ characteristics of epitaxial $YBa_2Cu_3O_x$ thin films have been made up to high resistance levels. We have found that the flux flow model of conventional pinning theory does not account for the dissipation at high currents in $YBa_2Cu_3O_x$. The observed power law behavior in the $I-V$ curves and the variation of the exponent with magnetic field are in agreement with a simple model based on dissipation caused by 2D vortices. Although a similar power law behavior has been reported previously, this study shows its validity at much higher magnetic fields and dissipation levels.

Acknowledgements

The work has been supported by the Director, Office of Basic Energy Sciences, Materials Sciences Division, of the US Dept. of Energy under contract No. DE-AC03-76SF00098. One of the authors (SKG) received financial support from USAID and Department of Science and Technology, Govt. of India, under the Indo–US Science and Technology Fellowship Program. GB acknowledges additional support from the Ford Foundation.

References

[1] R. Wordenweber, M.O. Abd-El-Hamed and J. Schneider, Physica C 171 (1990) 1.
[2] M. Tinkham, Introduction to Superconductivity (McGraw Hill, New York, 1975).
[3] Y.B. Kim, C.F. Hempstead and A.R. Strnad, Phys. Rev. 139 (1965) A1163.
[4] J. Ricketts, W.F. Vinen, J.S. Abell and T.C. Shields, Physica C 185–189 (1991) 2521.

[5] M.S. Colclough, J.S. Abell, C.E. Gough, J. Rickets, T. Shields, F. Wellhofer, W.F. Vinen, N.McN. Alford and T. Button, Cryogenics 30 (1990) 439.
[6] E. Zeldov, N.M. Amer, G. Koren, A. Gupta, M.W. McElfresh and R.J. Gambino, Appl. Phys. Lett. 56 (1990) 680.
[7] R.H. Koch, V. Folietti, W.J. Gallagher, G. Koren, A. Gupta and M.P.A. Fisher, Phys. Rev. Lett. 63 (1989) 1511.
[8] S.N. Artemenko, I.G. Gorlova and Yu.I. Latyshev, Physica C 193 (1992) 47.
[9] Masashi Ban, Tsuneo Ichiguchi and Toshiyuki Onogi, Phys. Rev. B 40 (1989) 4419.
[10] G.C. Yi, W. Jo, Y.K. Kim, T.W. Noh, D.K. Ko, H. Noh and Z.G. Khim, Physica C 194 (1992) 293.
[11] A. Iwase, N. Masaki, T. Iwata and T. Nihira, Physica C 174 (1991) 321.
[12] R. Wordenweber and M.O. Abd-El-Hamed, Supercond. Sci. Technol. 5 (1992) S113.
[13] M.V. Feigelman, V.B. Geshkenbein and A.I. Larkin, Physica C 167 (1990) 177.
[14] K. Shibutani, S. Hayashi, T. Egi, I. Shiigaki, R. Ogawa, Y. Kawate, K. Kitahama and S. Kawai, Physica C 185–189 (1991) 2277.
[15] W.C. McGinnis, E.W. Jacobs, C.D. Rees and T.E. Jones, Rev. Sci. Instrum. 61 (1990) 984.
[16] Teruo Matsushita and N.I. Baorong, Physica C 166 (1990) 423.
[17] M. Nahum, S. Verghese, P.L. Richards and K. Char, Appl. Phys. Lett. 59 (1991) 2034.
[18] F.P. Incropera and D.P. DeWitt, Introduction to Heat Transfer (Wiley, New York, 1990).
[19] Y.S. Touloukian, ed., Thermophysical Properties of Matter, vols. 2 and 5 (IFI/Plenum, New York, 1970).
[20] R.E. Russo, R.P. Reade, J.M. McMillan and B.L. Olson, J. Appl. Phys. 68 (1990) 1354.
[21] R. Wordenweber, M.O. Abd-El-Hamed and J. Schneider, J. Appl. Phys. 70 (1991) 2230.
[22] H.J. Jensen and P. Minnhagen, Phys. Rev. Lett. 66 (1991) 1630.
[23] K.H. Fischer, Physica C 193 (1992) 401.
[24] P.C.E. Stamp, L. Forro and C. Ayache, Phys. Rev. B 38 (1988) 2847.
[25] Q.Y. Ying and H.S. Kwok, Phys. Rev. B 42 (1990) 2242.
[26] L.C. Davis, M.R. Beasley and D.J. Scalapino, Phys. Rev. B 42 (1990) 99.
[27] S.N. Artemenko and A.N. Kruglov, Physica C 173 (1991) 125.
[28] A.M. Kadin, K. Epstein and A.M. Goldman, Phys. Rev. B 27 (1983) 6691.